

# Addition Spectra of Chaotic Quantum Dots: Interplay between Interactions and Geometry

Kang-Hun Ahn<sup>1</sup>, Klaus Richter<sup>1</sup>, and In-Ho Lee<sup>2</sup>

<sup>1</sup>*Max-Planck-Institut für Physik komplexer Systeme, Nöthnitzer Str. 38, 01187 Dresden, Germany*

<sup>2</sup>*School of Physics, Korea Institute for Advanced Study, Cheongryangri-dong, Seoul 130-012, Korea*  
(May 19, 2019)

We investigate the influence of interactions and geometry on ground states of clean chaotic quantum dots using the self-consistent Hartree-Fock method. We find two distinct regimes of interaction strength: While capacitive energy fluctuations  $\delta\chi$  follow approximately a random matrix prediction for weak interactions, there is a crossover to a regime where  $\delta\chi$  is strongly enhanced and scales roughly with interaction strength. This enhancement is related to the rearrangement of charges into ordered states near the dot edge. This effect is non-universal depending on dot shape and size. It may provide additional insight into recent experiments on statistics of Coulomb blockade peak spacings.

05.45.+b,72.10Fk,73.20.Dx

The understanding of the interplay between many-body interactions and chaos has evolved to a prominent field in mesoscopic physics. This challenging issue brings together two seemingly disconnected fields, namely many-particle physics and quantum chaos. Classically chaotic independent-particle dynamics is found in mesoscopics for both, disordered systems due to scattering at impurities and *clean* quantum dots, where the shape of the confining potential can give rise to chaotic electron motion. While interaction effects in disordered systems have been intensively studied in the recent past [1], accounts on the inter-relation between many-body effects and chaotic dynamics in ballistic quantum dots are still rare (see, e.g., Refs. [2,3]). The latter systems can be modelled by quantum billiards which have served as prototypes to investigate quantum signatures of integrable and chaotic single-particle dynamics [4]. Hence a generalization of these quantum chaos concepts to interacting particles in billiards appears natural. In this letter we approach this problem within a self-consistent Hartree-Fock (SCHF) approximation after checking its validity by comparing with exact diagonalization.

Our work was partly motivated by new measurements of charge transport through quantum dots with variable size and shape, which represent ideal tools to investigate experimentally interaction effects in confined chaotic systems. If such a dot with  $N$  electrons and ground state energy  $E_N$  is only weakly coupled to external leads a conductance peak is observed, upon tuning a gate voltage connected to the dot, whenever the chemical potential  $\mu_N = E_N - E_{N-1}$  coincides with that of the leads. In between the pronounced conductance peaks the current through the dot is suppressed due to Coulomb blockade [5]. The spacing between neighboring peaks as function of gate voltage is proportional to the capacitive energy

$$\chi_N = E_{N+1} - 2E_N + E_{N-1}. \quad (1)$$

A number of recent experiments [6–9] showed that fluctuations of  $\chi_N$  resemble a Gaussian distribution, while the

assumption of a constant interaction (CI), which properly describes the mean peak spacing, combined with random matrix theory (RMT), predicts a Wigner-Dyson distribution. Two reasons have been proposed for the Gaussian distribution, the scrambling of the single-particle spectrum due to interactions [6,10–13] and the deformation of the dot by changing the gate voltage [14].

However, it is not yet understood why the measured peak spacing fluctuations,  $\delta\chi = (\langle\chi_N^2\rangle - \langle\chi_N\rangle^2)^{1/2}$ , significantly vary between the different experiments: Patel et al. [8] found rather small fluctuations which are comparable to the mean level spacing  $\Delta$  of the independent-particle eigenstates. They are in line with the RMT+CI model predicting  $\delta\chi = \Delta(4/\pi - 1)^{1/2} \simeq 0.52\Delta$ , and with RPA calculations for weak interactions (high densities,  $r_s < 1$ ) [15,16]. On the contrary, the other experiments yield large fluctuations which scale rather with  $\langle\chi_N\rangle$  than with  $\Delta$ :  $\delta\chi \approx 0.06 - 0.15\langle\chi_N\rangle$  in Ref. [6,7,9]. E.g., in the recent experiment [9] on a silicon sample, where the shape of the dot is expected not to be distorted by tuning the gate voltage,  $\delta\chi$  was found to be 15 times larger than predicted by RMT.

Thus two main open questions arise: (i) what is the responsible mechanism for the large fluctuations and (ii) why do they show such a sample-dependent behavior, assuming that the samples are chaotic?

Here we consider clean chaotic quantum dots and study the interplay between the Coulomb interaction of the electrons and the geometry of the dots. We propose a mechanism for enhanced capacitive energy fluctuations  $\delta\chi$  in chaotic structures and show that:

- (i) interaction drives the systems to a regime of large, non-universal fluctuations by developing ordered charge states near the edges.
- (ii) the shape of the confinement is an important factor for the formation of such states and hence for the fluctuations.

To our knowledge, all related theoretical studies con-

sider interaction effects for disordered models [6,10–13], apart from the work by Stopa [2], who suggested the occurrence of strongly scarred states as a mechanism for enhanced fluctuations. Our calculations show that  $\delta\chi$  can be enhanced in the absence of scarred states, and it seems unclear whether they can survive for stronger interactions.

We model the quantum dots by a family of billiards which arise from a deformation of the disk [17]. They have already been employed as non-interacting models in the context of Coulomb blockade [14,18]. Here they will serve as appropriate tools to study systematically effects of electron interaction upon changing the billiard geometry. The confinement is defined by a hardwall potential  $U$  satisfying  $U(u, v) = 0$  inside a singly-connected domain  $D$  and  $U(u, v) = \infty$  outside. Using complex coordinates  $\omega = u + iv$  and  $z = x + iy$ ,  $D$  is defined by the conformal mapping [17]

$$\omega(z) = R \frac{z + bz^2 + ce^{i\delta}z^3}{\sqrt{1 + 2b^2 + 3c^2}} \quad ; \quad |z| < 1. \quad (2)$$

The real parameters  $b, c$ , and  $\delta$  determine the shape, and  $R$  defines the dot size and area,  $A = \pi R^2$ . For the deformations to be considered (see insets in Fig. 2) the classical independent-particle dynamics is predominantly chaotic (described by a large Kolmogorov entropy for the strongest deformation [18]), and we found that the single-particle energies exhibit Wigner-Dyson statistics.

To include interactions we first calculate the single-particle eigenstates and -energies  $\epsilon_i$  of a deformed billiard and use them to construct the Coulomb interaction matrix  $V_{ijkl}$  and the many-electron Hamiltonian

$$H = \sum_i \epsilon_i c_i^\dagger c_i + \frac{1}{2} \sum_{ijkl} V_{ijkl} c_i^\dagger c_j^\dagger c_l c_k. \quad (3)$$

Here  $c_i^\dagger(c_i)$  creates (annihilates) the  $i$ -th eigenstate of the non-interacting Hamiltonian. In terms of energy units  $\hbar^2/(2m^*R^2)$ ,  $V_{ijkl}$  is proportional to the dimensionless interaction strength, or system size,  $R/a_B^*$ , where  $a_B^* = \hbar^2\epsilon/m^*e^2$  is the effective Bohr radius of the host material.

Eq. (3) can serve as a starting point for both exact diagonalization and SCHF calculations. Using exact diagonalization for up to 5 particles we have studied the level statistics of highly *excited* many-body states in chaotic geometries and find with increasing interaction a transition from Poisson- to Wigner-Dyson-type behavior [19].

In this work we focus on *ground state* properties for many-electron quantum dots and use SCHF for systems up to 27 spinless electrons. The SCHF allows us to calculate the ground state energies even in the presence of two-electron density correlations which are ignored in the RPA perturbation calculations [15,16]. To check the validity of our SCHF results we first compare the respective capacitive energies with the exact diagonalization results

for few electrons. As shown in Fig. 1 the SCHF results are very accurate even for strong interactions. We expect the SCHF results to be also accurate for larger electron number.

The numerical SCHF results for  $\chi_N$  did not show any visible dependence on  $N$  but rather on the interaction strength (system size)  $R/a_B^*$ . Let us thus consider the mean fluctuations  $\delta\chi$ , where the statistical average  $\langle \dots \rangle$  is performed over  $N$  as in the experiments [6–9].

Our main results are summarized in Fig. 2. It shows  $\delta\chi$  as a function of interaction strength for three different geometries depicted as insets close to the curves. For small size quantum dots,  $R/a_B^* \lesssim 12$ ,  $\delta\chi$  fluctuates around the constant RMT+CI value ( $\approx 0.52\Delta$ ). Most interestingly, we find for larger  $R/a_B^*$  a *cross-over* to a regime where the capacitive energy fluctuations increase roughly linearly with increasing interaction strength. To our knowledge such a clear-cut cross-over behavior has not been found in any tight-binding model for disordered systems. This implies that the absence of a disorder potential and/or the effect of the confinement on the charge distribution in the dots could be responsible.

Using the standard definition of  $r_s$ , namely  $r_s^2 = A/(\pi N a_B^{*2})$ , without relying on its physical interpretation for short-ranged interaction, we have  $r_s = (R/a_B^*)/\sqrt{N}$ . Since we calculate  $\delta\chi$  over a range  $3 \leq N \leq 27$  for a given value of  $R/a_B^*$  in Fig. 2,  $r_s$  has not a well-defined value but is in the range  $(1/\sqrt{27})R/a_B^* \leq r_s \leq (1/\sqrt{3})R/a_B^*$ . Hence the cross-over value of  $R/a_B^*$  in Fig. 2 implies that  $\delta\chi$  retains its RMT value up to  $r_s \approx 2$  which is consistent with the RPA approach of Ref. [15].

In the following we discuss the mechanism responsible for the cross-over behaviour of  $\delta\chi$ . To this end it proves convenient to decompose  $\chi_{N-1}$  as [15]

$$\chi_{N-1} \simeq \left[ \epsilon_{N+2}^{(N+1)} - \epsilon_{N+2}^{(N)} \right] + \left[ \epsilon_{N+2}^{(N)} - \epsilon_{N+1}^{(N)} \right] \equiv E_1 + E_2. \quad (4)$$

Here,  $\epsilon_j^{(i)}$  denotes the  $j$ -th eigenvalue of the SCHF Hamiltonian with  $i$  electrons. Quantitatively, Eq. (4), which relies on Koopmans' approximation, does not give the same value as  $\delta\chi$  in Fig. 2. However, Eq. (4) shows qualitatively the same behaviour with the same cross-over point but slightly larger slope than in the SCHF case, Fig. 2.

The quantity  $E_1$  in Eq. (4), which describes the interaction energy between the electrons in  $(N+1)$ th and  $(N+2)$ th state, has been considered in detail in Ref. [15].  $E_2$  is the energy difference between two adjacent single-particle levels of the same Hamiltonian. In the RPA approach of Ref. [15] it was claimed that  $\langle E_2 \rangle$  is given by  $\Delta$  and its fluctuations follow the RMT value  $\simeq 0.52\Delta$ . As displayed in the inset of Fig. 2 our calculations show that this seems to be true for  $R/a_B^* \lesssim 12$ , which includes the regime  $r_s < 1$ , where RPA is reliable. However,  $\langle E_2 \rangle/\Delta$  grows as the system size increases, and its fluctuations  $\delta E_2/\Delta$  and  $\delta E_2/\langle E_2 \rangle$  do no longer follow the RMT prediction for  $R/a_B^* \gtrsim 12$ .

The similarity of the cross-over behavior of  $\delta\chi$  and  $\delta E_2$  in Fig. 2 suggests that an analysis of  $E_2$  proves appropriate and sufficient to understand the enhanced fluctuations  $\delta\chi$ . However, we note that the underlying mechanism to be discussed is more general.

What happens in the regime  $R/a_B^* \gtrsim 12$ ? To answer this question we present in Fig. 3 the evolution of unoccupied SCHF single-particle levels  $\epsilon_n^{(N)}$ ,  $n=N+1, N+2, \dots$  with increasing interaction for a few representative values of  $N$ . We find that the enhancement of mean and rms values of  $E_2 = (\epsilon_{N+2}^{(N)} - \epsilon_{N+1}^{(N)})$  is accompanied by the appearance of sudden jumps of the single particle levels as marked by vertical arrows in Fig. 3. (Note however that not for all values of  $N$  the energy levels show such jumps in the  $R/a_B^*$  range considered, e.g.  $N=16$ .)

The abrupt changes in the SCHF single-particle energies go along with a rearrangement of the corresponding wavefunctions as shown in Fig. 4(a,b). This indicates a change in the underlying mean-field potential and thereby in the total charge densities. The two lower left (right) panels in Fig. 4 depict the total charge densities for interaction strength  $R/a_B^* = 5$  (15) for two selected, representative  $N$ . A systematic analysis of a large number of geometries and particle numbers allowed us to extract two common trends visualized in the figure: (i) With growing system size the electrons tend to be localized near the edge of the dot. *For  $R/a_B^* \gtrsim 12$  the electric charges are reorganized in an ordered structure similar to a one-dimensional crystal or a charge density wave state.* (ii) An abrupt change in the mean-field potential for fixed  $N$  occurs when an electron from the inner region of the dot moves into a state close to the edge.

Let us discuss the connection to the increase in  $\langle E_2 \rangle$  and  $\delta E_2$ . Electrons in states, which extend over the whole chaotic dot for small  $R/a_B^*$ , move with increasing interaction to the edge due to the long-range Coulomb repulsion. When the states near the edge are fully occupied (see e.g. Fig. 4 (d)) the corresponding mean field reduces the accessible space for the next electron above the Fermi level (crossover from Fig. 4 (a) to (b)). The reduced effective size of the dot gives rise to an enhanced level spacing  $\langle E_2 \rangle$  which is also accompanied by enhanced fluctuations. Note that  $\delta E_2 / \langle E_2 \rangle$  also deviates from the RMT value of  $\approx 0.52$ , which indicates that *the HF single-particle states near the Fermi level do no longer follow the RMT in the strong interaction regime even for the chaotic geometry due to the charge reorganization near the edge.*

The reorganized charge states near the edge differ from a Wigner crystal where the electrons are localized in two-dimensional space due to electron correlations [20]. The charge rearrangement considered here results from the competition between the long-range interaction and the confinement potential. For smaller  $N$  a phase which might be called a ‘‘crystal chain’’ evolves where the elec-

trons are well localized near the edge with clear spatial separation (see, e.g., Fig. 4(d)). It can be argued that due to quantum fluctuations of the 1D crystal lattice this phase will be bounded from above by some critical electron number  $N_c$ . Since the minimum distance between electrons should be larger than a Fermi wavelength  $\lambda_F$ , the maximum number of electrons which can reside at the edge is  $\approx L_p / \lambda_F$ , where  $L_p$  is the perimeter of the dot. Since in the crystal chain state all electrons are at the edge, the number  $N_c$  for the crystal chain can be estimated as

$$N_c \approx L_p^2 / A, \quad (5)$$

where we used  $\lambda_F \approx R / \sqrt{N}$ . For the dot geometries defined by Eq. (2) we find  $N_c$  to be of order of 10. This rough estimation is in line with our numerical results where for  $N = 7$  all electrons are near the edge, whereas for  $N = 11$  only 10 electrons seem close to the edge with one electron near the center of the dot (see Fig. 4). For this case,  $N > N_c$ , the charge density exhibits a modulation along the edge rather than well separated charges. States similar to those were previously found using a spin-density-functional theory for circular and elliptic geometries and were coined rotational charge density wave states [21]. While the formation of the crystal chain is responsible for the enhanced fluctuations at small electron numbers  $\sim 10$ , the appearance of the rotational charge density wave states plays the same role for the enhancement for larger electron numbers (see, e.g., Fig. 3 for  $N=24$ ).

A few further remarks are due:

(i) The kink in the geometry of the strongly deformed dot (bottom inset in Fig. 2) renders the formation of edge states more difficult than in the dot with a shape close to a disk. This is the reason why the fluctuations  $\delta\chi$  are the largest in the latter case and turn out to be system dependent, even if the non-interacting geometries all exhibit chaotic dynamics. Moreover, the wavefunctions of the ordered edge states do no longer follow RMT predictions.

(ii) The accumulation of charge near the edge alone is not enough to produce enhanced fluctuations  $\delta\chi$ . As visible in Fig. 4(c, e) the weakly interacting dots ( $R/a_B^*=5$ ) also show charge enhancement near the edge, but  $\delta\chi$  is still similar to the RMT value. This can be understood within the RPA approach of Ref. [15], where the corresponding contribution to  $\delta\chi$  was shown to be of order  $\sim g^{-1/2} \Delta$  where  $g \gg 1$  is the dimensionless conductance.

(iii) The interesting problem to find a phase diagram of the quantum dot as a function of system size, shape, and  $N$  is beyond the scope of this work. We can state at least that for  $N < 30$  the border between irregular states showing RMT like behaviour and the reorganized charge states is not simply given by a critical value of  $r_s$  alone.

(iv) The experimental observation of the cross-over

behavior of  $\delta\chi$  from a constant to a roughly linear increase would be most interesting. For GaAs samples with  $a_B^* \approx 10$  nm, the cross-over may appear for a system size close to  $0.1\mu\text{m}$ . With regard to the crystal chain states recent experiments [22] on quantum dots with small number of electrons with and without spatial symmetry are expected to be a good testing ground.

To conclude, we considered interaction effects in clean chaotic quantum dots. We propose as a mechanism for enhanced capacitive energy fluctuations the formation of ordered charge states near the edge of quantum dots. In the regime where the ordered states are developed, the fluctuations are system-dependent and sensitive to the shape, even in chaotic geometries.

We thank R. Berkovits, H. Castella, A. Cohen, Y. Gefen, S. Kettman, A.D. Mirlin, G. Montambaux, and J.-L. Pichard for helpful discussions. KHA also thanks M. Takahashi for useful comments on numerical calculations.

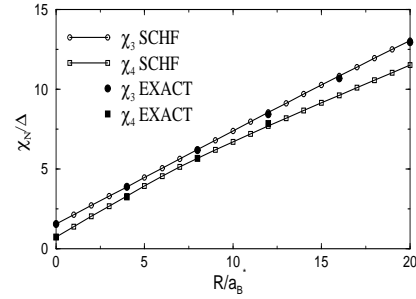


FIG. 1. Comparison of self-consistent Hartree-Fock (SCHF) and exact diagonalization (EXACT) results of capacitive energies  $\chi_N$ , Eq. (1), as a function of interaction strength for  $N=3$  (upper) and  $N=4$  (lower curve) for the billiard geometry shown in the bottom inset of Fig. 2.

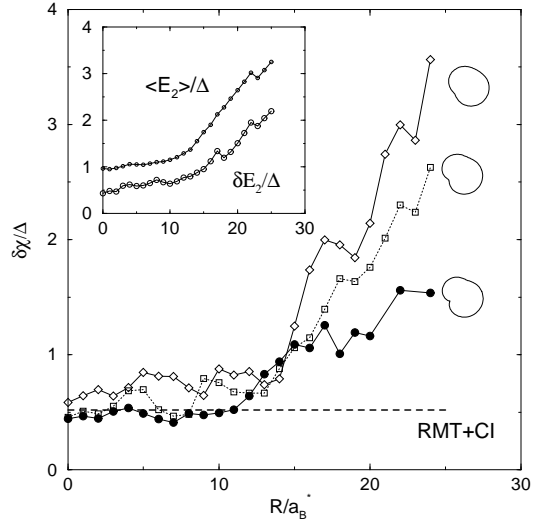


FIG. 2. Fluctuations of capacitive energies  $\delta\chi = (\langle\chi_N^2\rangle - \langle\chi_N\rangle^2)^{1/2}$  as a function of interaction strength for interacting electrons in three chaotic billiards of different shape shown on the right (defined via Eq. (2) with  $\delta = 1.5$ ,  $b = c = 0.12, 0.16$ , and  $0.2$  from above).  $\delta\chi$  shows a clear cross-over near  $R/a_B^* = 12$  and increases with increasing  $R/a_B^*$  in the strong interaction regime. Inset: The mean and rms value of  $E_2 = \epsilon_{N+2}^{(N)} - \epsilon_{N+1}^{(N)}$  for the quantum dot of the bottom right inset. Note that for larger interactions  $\langle E_2 \rangle \neq \Delta$ .

- 
- [1] For a recent collection of papers see, e.g., *Annalen der Physik*, **7** (5-6) (1998).
  - [2] M. Stopa, *Physica B* **251**, 228 (1998).
  - [3] D. Ullmo, H.U. Baranger, K. Richter, F. von Oppen, and R.A. Jalabert, *Phys. Rev. Lett.* **80**, 895 (1998).
  - [4] *Chaos and Quantum Physics*, M.J. Giannoni, A. Voros, and J. Zinn-Justin, eds. (North-Holland, New York, 1991).
  - [5] M.A. Kastner, *Rev. Mod. Phys.* **64**, 849 (1992).
  - [6] U. Sivan *et al.*, *Phys. Rev. Lett.* **77**, 1123 (1996).
  - [7] F. Simmel *et al.*, *Europhys. Lett.* **38**, 123 (1997).
  - [8] S. R. Patel *et al.*, *Phys. Rev. Lett.* **80**, 4522 (1998).
  - [9] F. Simmel *et al.*, *Phys. Rev. B* **59**, R10441 (1999).
  - [10] A. Cohen, K. Richter, and R. Berkovits, *Phys. Rev. B* (in press).
  - [11] S. Levit and D. Orgad, cond-mat/9901298.
  - [12] L. Bonci and R. Berkovits, cond-mat/9901332.
  - [13] P. N. Walker, Y. Gefen, and G. Montambaux, cond-mat/9902099.
  - [14] R. O. Vallejos, C. H. Lewenkopf, and E. R. Mucciolo, *Phys. Rev. Lett.* **81**, 677 (1998).
  - [15] Ya. M. Blanter, A. D. Mirlin, and B. A. Muzykanskii, *Phys. Rev. Lett.* **78**, 2449 (1997).
  - [16] R. Berkovits and B. L. Altshuler, *Phys. Rev. B* **55**, 5297 (1997).
  - [17] M. V. Berry and M. Robnik, *J. Phys. A* **19**, 649 (1986).
  - [18] H. Bruus and A. D. Stone, *Phys. Rev. B* **50**, 18275 (1994).
  - [19] K.-H. Ahn and K. Richter (unpublished).
  - [20] A. A. Koulakov and B. I. Shklovskii, *Phys. Rev. B* **57**, 2352 (1998).
  - [21] K. Hirose and N. S. Wingreen, *Phys. Rev. B* **59**, 4604 (1999).
  - [22] S. Tarucha *et al.*, *Phys. Rev. Lett.* **77**, 3613 (1996); D.

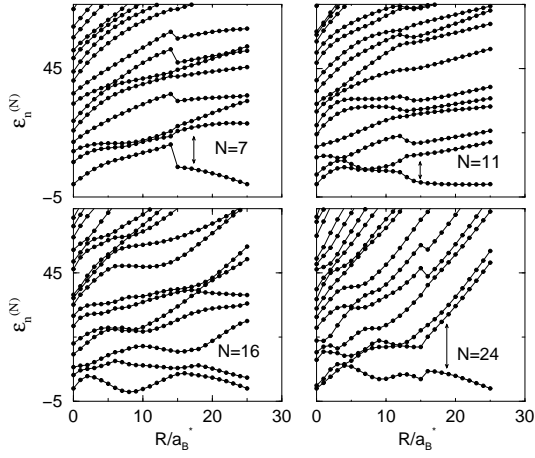


FIG. 3. Unoccupied SCHF levels  $\epsilon_n^{(N)}$ ,  $n = N + 1, N + 2, \dots$  as a function of interaction strength for a chaotic quantum dot (bottom right inset in Fig. 2) with  $N = 7, 11, 16,$  and  $24$  electrons. Note the sudden jumps in the level spacings  $E_2$  between the lowest two adjacent levels which are caused by abrupt changes in the mean-field potential. For clarity, the levels in each panel are shifted by an amount  $a(N) + b(N)R/a_B^*$ . The energy units are  $\hbar^2/(2m^*R^2)$ .

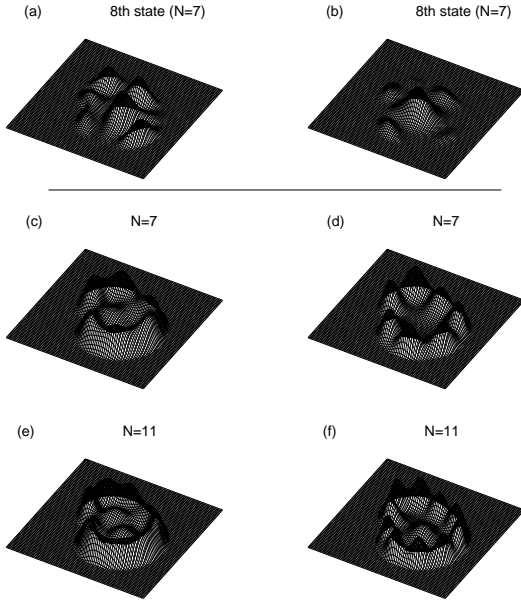


FIG. 4. Charge reordering with increasing interaction for a chaotic dot (bottom inset in Fig. 2);  $R/a_B^* = 5$  (15) in left (right) panels. Panels (a) and (b) show the probability density of the first unoccupied SCHF single-particle state  $n = 8, N = 7$  (lowest curve in upper left panel, Fig. 3). In (c) to (f) the total charge densities for  $N = 7, 11$  are displayed.